Supporting Information for

Hypoxia-responsive luminescent CEST MRI agent for *in vitro* and *in vivo* tumor detection and imaging

Sanu Karan[1,2,†], Mi Young Cho[1,†], Hyunseung Lee[1], Hye Sun Park[1], Eun Hee Han[1], Youngkyu Song[3], Youlee Lee[3], Mina Kim[4], Jee-Hyun Cho[3,*], Jonathan L. Sessler[5,*], Kwan Soo Hong[1,2,*]

[1]Research Center for Bioconvergence Analysis, Korea Basic Science Institute, Cheongju 28119, Korea
[2]Graduate School of Analytical Science and Technology, Chungnam National University, Daejeon 34134, Korea
[3]Research Equipment Operations Division, Korea Basic Science Institute, Cheongju 28119, 34134, Korea
[4]Department of Neuroinflammation, UCL Queen Square Institute of Neurology, Faculty of Brain Science, London WC1N 3BG, United Kingdom
[5]Department of Chemistry, The University of Texas at Austin, Austin, Texas 78712-1224, USA

[†]These authors contributed equally to this work

*To whom correspondence should be addressed: jhcho@kbsi.re.kr (J.-H. Cho), sessler@cm.utexas.edu (J.L. Sessler), kshong@kbsi.re.kr (K.S. Hong).

Table of contents

Materials, methods, and instrumentation

Analytical grade chemicals sourced as follows were used without further purification: 3-Nitrophthalic anhydride (compound **1**, TCI), ethanolamine (Sigma Aldrich), triphenylphosphine (Sigma Aldrich), N-bromosuccinimide (Sigma Aldrich), potassium carbonate (Sigma Aldrich), *t*-butyl bromoacetate (Sigma Aldrich), 1-(3-dimethylaminopropyl)-3-ethylcarbodiimide hydrochloride (Carbosynth), 1,4,7,10-tetraazacyclododecane (TCI), trifluoroacetic acid (TCI), europium(III) chloride hexahydrate (Sigma Aldrich), nitroreductase from *escherichia coli* (Sigma), *beta*-nicotinamide adenine dinucleotide disodium salt (TCI), N,N-dimethylformamide (Sigma Aldrich), tetrahydrofuran (Sigma Aldrich), plasma (Sigma), and dimethyl sulfoxide (Sigma Aldrich). Column chromatography was performed using silica gel 60 (70–230 mesh) as the stationary phase. Analytical thin layer chromatography was performed using silica gel 60 (pre-coated sheets with 0.25 mm thickness). Compounds were characterized by ^{1}H- and ^{13}C-NMR spectroscopy, and high-resolution (HRMS), and electrospray ionization (ESI) mass spectrometry. NMR spectra were collected on a 400 MHz spectrometer (Bruker, Germany), using tetramethylsilane (TMS) as the internal standard (0 ppm) and DMSO-d_6 as the solvent. Mass spectra were obtained on a Synapt G2-HDMS instrument (Waters, Manchester, UK) equipped with the MassLynx 4.1 software. The hypoxia chamber used in this study was purchased from Billps-Rothenberg (Del Mar, CA, USA).

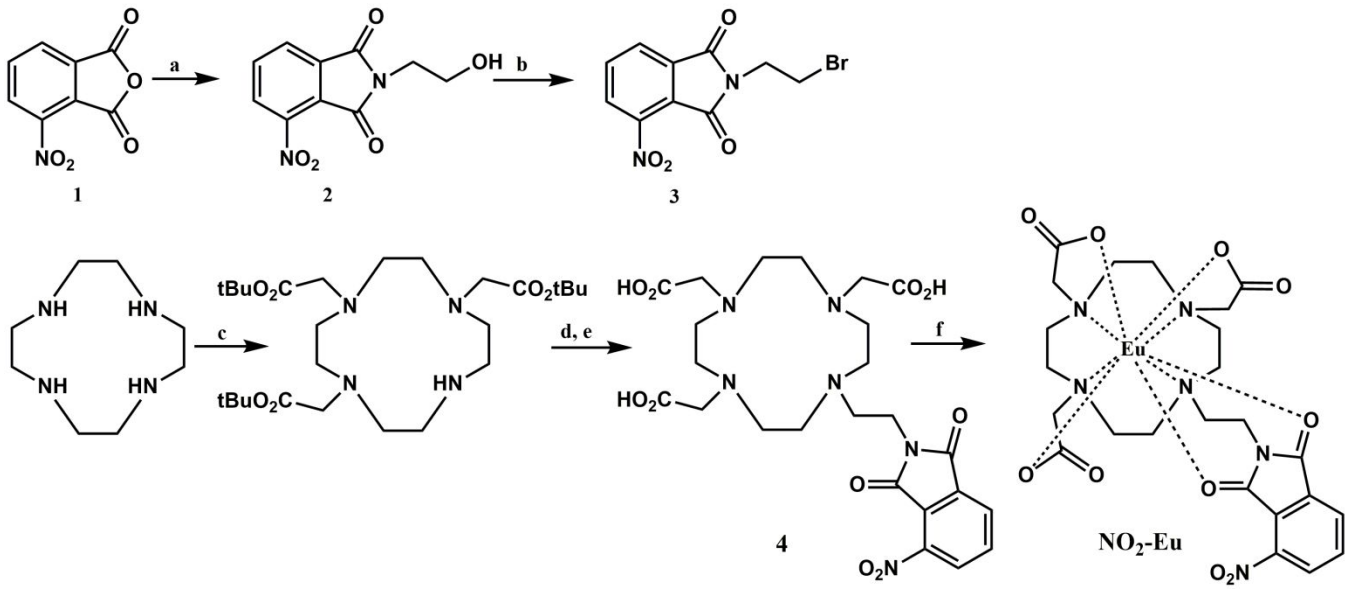

Scheme S1. Synthetic approach to the nitroreductase (NTR)-activated bimodal **NO_2-Eu** probe. (a) Ethanolamine, dimethylformamide (DMF) at 85°C, 24 h; (b) N-bromosuccinimide (NBS), PPh_3, DMF at 80°C, 16 h; (c) *t*-butyl bromoacetate, K_2CO_3, DMF at 75°C, 18 h; (d) compound **3**, K_2CO_3, DMF at ~90°C, 16 h; (e) trifluroacetic acid (TFA), room temperature, 24 h; (f) $EuCl_3 \cdot 6H_2O$.

Synthesis of compounds 2-4

A dimethylformamide (DMF) solution (5 mL) of 3-nitrophthalimide (Scheme S1, compound **1**, 193 mg, 1.0 mM) and ethanolamine (122 mg, 2 mM) were stirred at 85°C under a nitrogen atmosphere for 24 h. The reaction mixture was diluted with water and extracted with EtOAc. After collection of the organic layer and removal of the bulk of the solvent under reduced pressure, the crude compound was purified by silica gel column chromatography using ethyl acetate / hexanes (EtOAc/Hex) (1:1) as the eluent; this afforded 198 mg (83.9%) of compound **2**. ^{1}H NMR (400 MHz, $CDCl_3$): δ 8.062 (d, J = 3.68, 1H); 8.043 (d, J = 4.32, 1H); 7.882 (t, J = 7.76,7.8 1H); 3.843 (m, 4H); 2.2364 (s, 1H). ^{13}C NMR (100 MHz, $CDCl_3$): 166.253, 163.352, 145.066, 135.524, 134.020, 128.646, 127.177, 123.716, 77.070, 60.317, 41.246 ppm. ESI HR-MS m/z (M+Na): calcd. 259.03, found 259.033.

A dimethylformamide (DMF) solution (5 mL) of compound **2** (Scheme S1, 236 mg, 1.0 mM) and triphenylphosphine (917 mg, 3.5 mM) were stirred at 0°C under a nitrogen atmosphere for 10 min. Then N-bromosuccinimide (445 mg, 2.5 mM) in 3 mL DMF was added slowly to the reaction mixture, which was stirred at 80°C overnight. The reaction mixture was diluted with water and extracted with EtOAc. After collection of the organic layer and removal of the bulk of the solvent under reduced pressure, the crude compound was purified by silica gel column chromatography using ethyl acetate / hexanes (EtOAc/Hex) (1:2) as the eluent; this afforded 224 mg (74.9%) of compound **3**. ^{1}H NMR (400 MHz, $CDCl_3$): δ 8.184 (d, J = 7.8, 2H); 7.993 (t, J = 7.76, 7.8 1H); 4.191 (t, J = 6.52, 2H); 3.6769 (t, J = 6.76, 2H); ^{13}C NMR (100 MHz, $CDCl_3$): 165.304, 162.461, 145.226, 135.657, 133.859, 128.881, 127.365, 123.577, 39.948, 27.727 ppm. ESI HR-MS m/z (M+H): calcd. 298.96, found 298.967.

A dimethylformamide (DMF) solution (5 mL) of DO3A (Scheme S1, 515 mg, 1.0 mM) and K_2CO_3 (672 mg, 2 mM) were stirred at 0°C under a nitrogen atmosphere for 15 min. Then compound **3** (449 mg, 1.5 mM) dissolved in 3 mL DMF was added slowly to the reaction mixture, which was then stirred at 85-

90°C for 16 h. After this time, the reaction mixture was diluted with water and extracted with EtOAc. After collection of the organic layer and removal of the bulk of the solvent under reduced pressure, the crude compound was dissolved in trifluoroacetic acid (TFA) and stirred for 24 h. The mixture was then evaporated to dryness and purified by silica gel column chromatography using ethyl acetate/hexanes (EtOAc/Hex) (2:1) as the eluent; this afforded 419 mg (74.2%) of compound **4**. ^{1}H NMR (400 MHz, DMSO-d_6): δ 8.318 (d, J = 8.24, 1H); 8.263 (t, J = 7.84, 8.12 1H); 8.086 (d, J = 7.4, 1H); 5.350 (s, 2H); 3.696 (d, J = 4.56); 3.363 (d, J = 8.12, 6H); 3.343 (m, 16H); ^{13}C NMR (100 MHz, DMSO-d_6): 167.417, 164.612, 144.365, 136.370, 129.560, 127.939, 65.974, 53.835, 49.382, 32.967 ppm. ESI HR-MS m/z (M+H): calcd. 565.22, found 565.225.

Synthesis of NO_2-Eu

The free ligand (compound **4**) (0.056 g, 0.1 mmol) and K_2CO_3 (41 mg, 0.03 mM) were dissolved in water (10 mL) and the pH was adjusted to 7 with NaOH (0.1 M). To this solution was added excess $EuCl_3 \cdot 6H_2O$. The pH was adjusted to 6.5 by adding 0.01 M HCl and the resulting mixture allowed to stir at room temperature for 12 h. The pH was increased above 8 using 1 M aqueous NaOH, which caused the excess Eu^{3+} to precipitate as $Eu(OH)_3$. The solution was filtered and the pH was readjusted to 7 using 1 M HCl. The solution obtained in this way was freeze-dried to give the desired complex. An aqueous solution of the **NO_2-Eu** complex was examined for the absence of free Eu^{3+} ion using the xylenol orange indicator test. HPLC purity was measured on a Sunfire C18 column (4.6 mm × 150 mm, 5 μm; Waters, MA, USA) at 1/min flow rate and giving a retention time for probe **NO_2-Eu** of R_f = 3.2 min. On this basis the purity of probe **NO_2-Eu** was estimated to be 95.2%. ESI HR-MS m/z (M+2Na): calcd. 763.10, found 763.110.

The linear range and detection limit

The detection limit of probe **NO_2-Eu** toward NTR was calculated based on fluorescent spectroscopic titrations. The emission spectrum of the probe (2 μM) was measured ten times. The standard deviation of the blank solution was also measured. The emission intensity (λ_{em} = 512 nm) of probe **NO_2-Eu** was plotted vs. the concentrations of NTR. The detection limit was calculated using the following equation: detection limit = 3σ/k, where σ is the standard deviation of the blank measurement, and k is the slope between the luminescence intensity versus the NTR concentration.

NTR detection assay using high performance liquid chromatography (HPLC)

HPLC was performed using an HPLC system (YL9100, Youngin, Seoul, South Korea) with a Sunfire C18 column (4.6 mm × 150 mm, 5 μm, Waters, Massachusetts, USA). The conditions were as follows: Volume ratio of acetonitrile/H_2O = 30:70 (0 min) to 5:95 (10 min); flow rate 1 mL/min; UV detection at ≤254 nm.

Bacterial strains and cell culture conditions

Colonies of the *E. coli* strain (KCTC 1682) were grown in Luria Bertani (LB) broth (Difco, Franklin Lakes, NJ, USA) through the exponential phase at 37°C on a shaker (200 rpm). The murine colon cancer cell line CT26 provided by Y. S. Gho (POSTECH, Korea) was cultured in Minimum Essential Media (MEM, Gibco, Grand Island, NY, USA) containing 10% fetal bovine serum (FBS, Gibco) and 1% antibiotic-antimycotic (Gibco). The cells were maintained in a humidified incubator containing 5% CO_2 at 37°C.

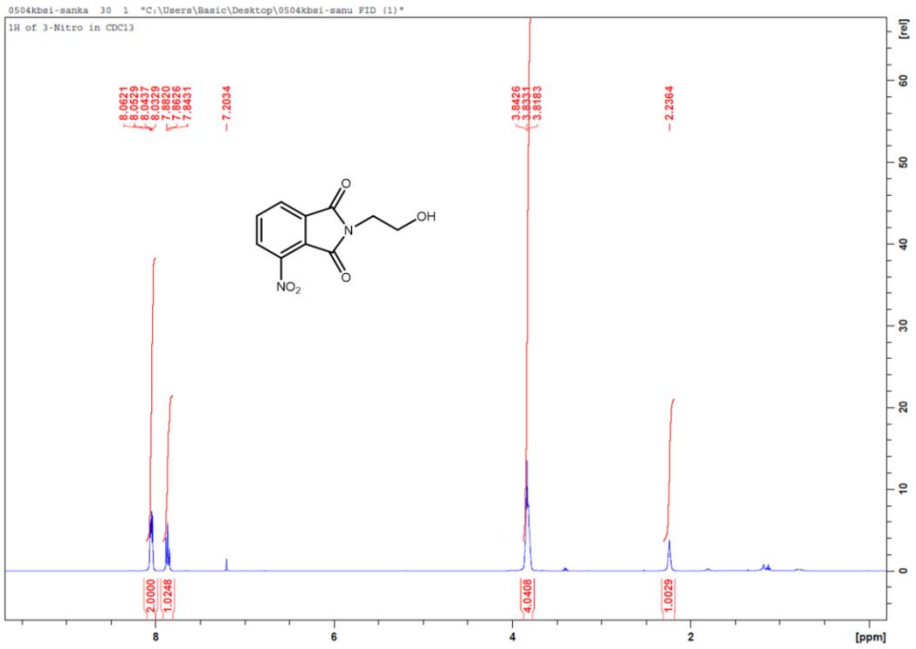

Figure S1. ^{1}H NMR spectrum of compound **2** in $CDCl_3$.

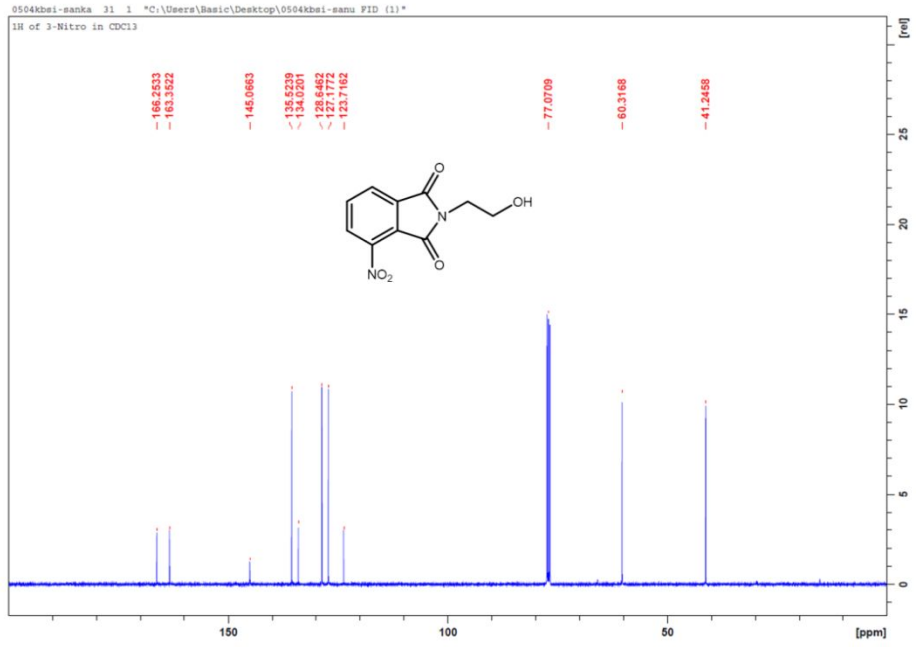

Figure S2. ^{13}C NMR spectrum of compound **2** in $CDCl_3$.

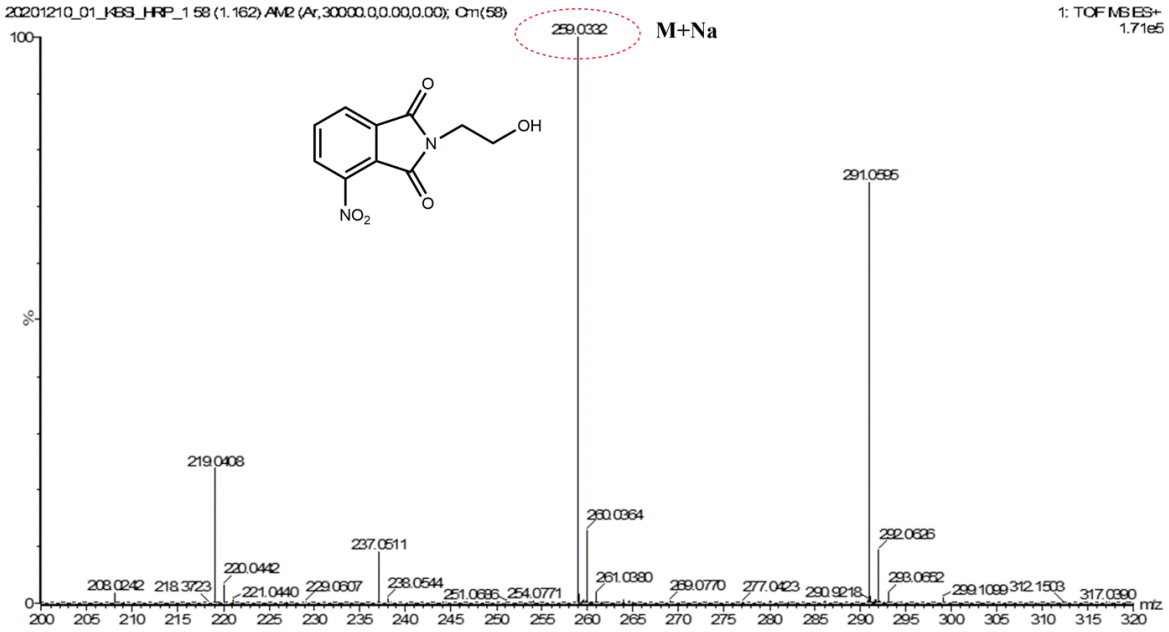

Figure S3. HRMS ESI spectrum of compound **2**.

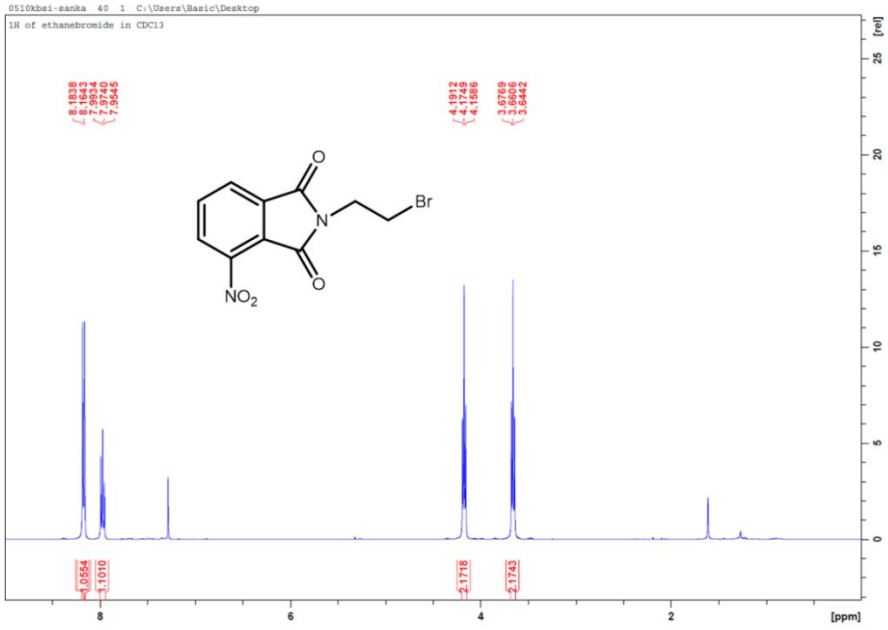

Figure S4. ^{1}H NMR spectrum of compound **3** in $CDCl_3$.

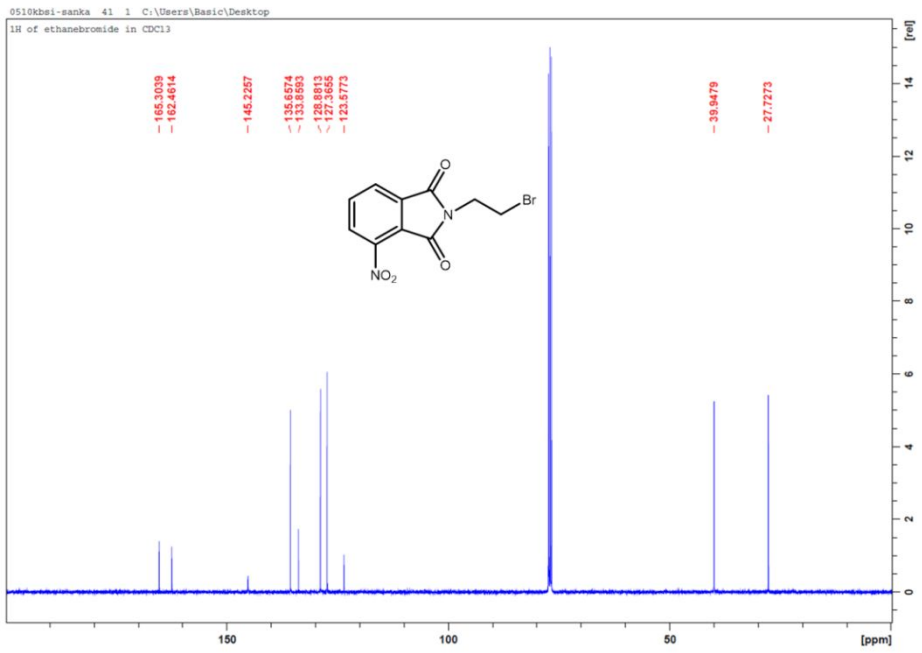

Figure S5. ^{13}C NMR spectrum of compound **3** in $CDCl_3$.

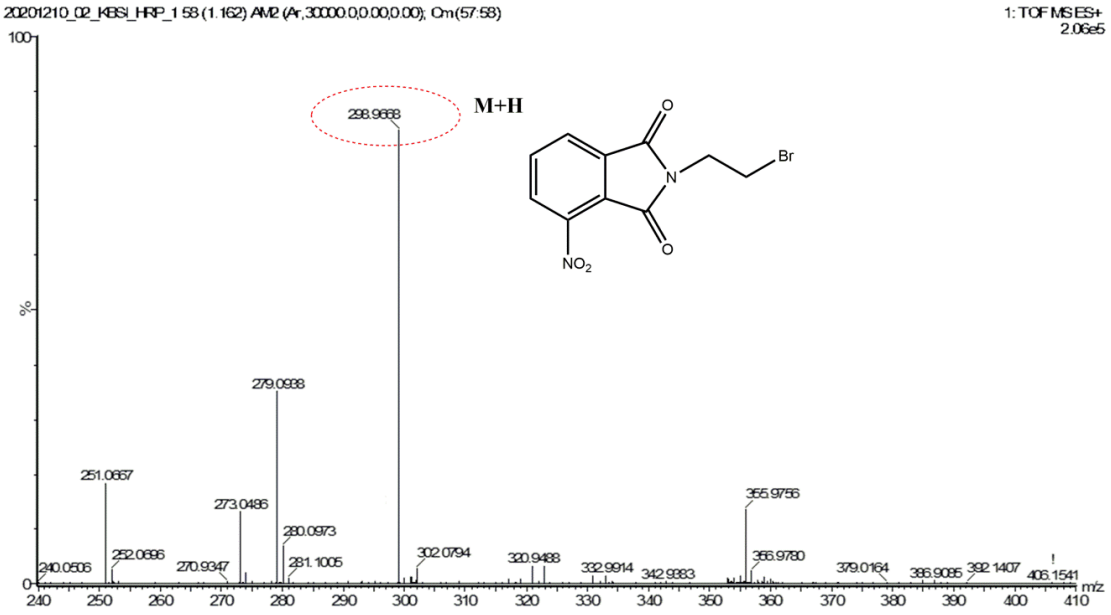

Figure S6. HRMS ESI spectrum of compound **3**.

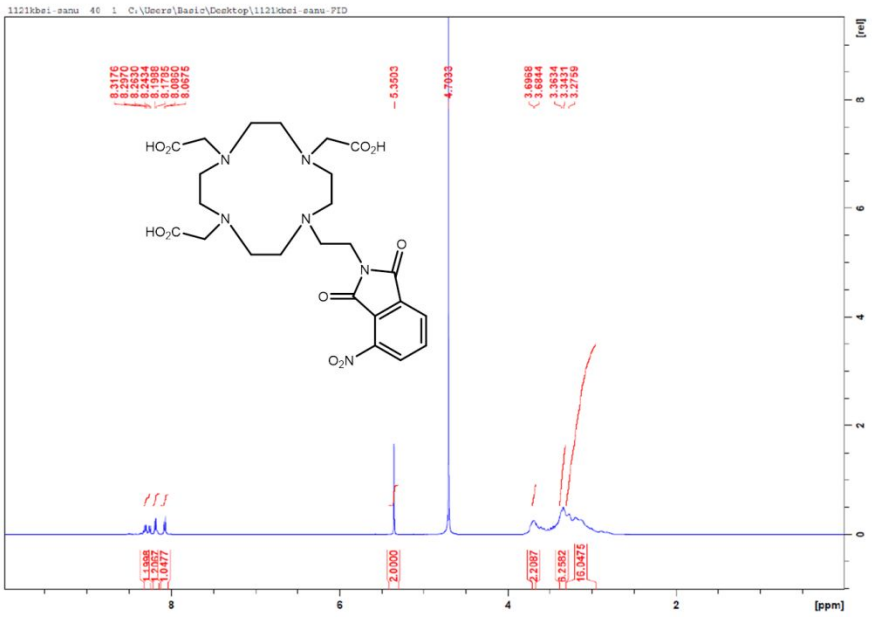

Figure S7. ^{1}H NMR spectrum of compound **4** in DMSO-d_6.

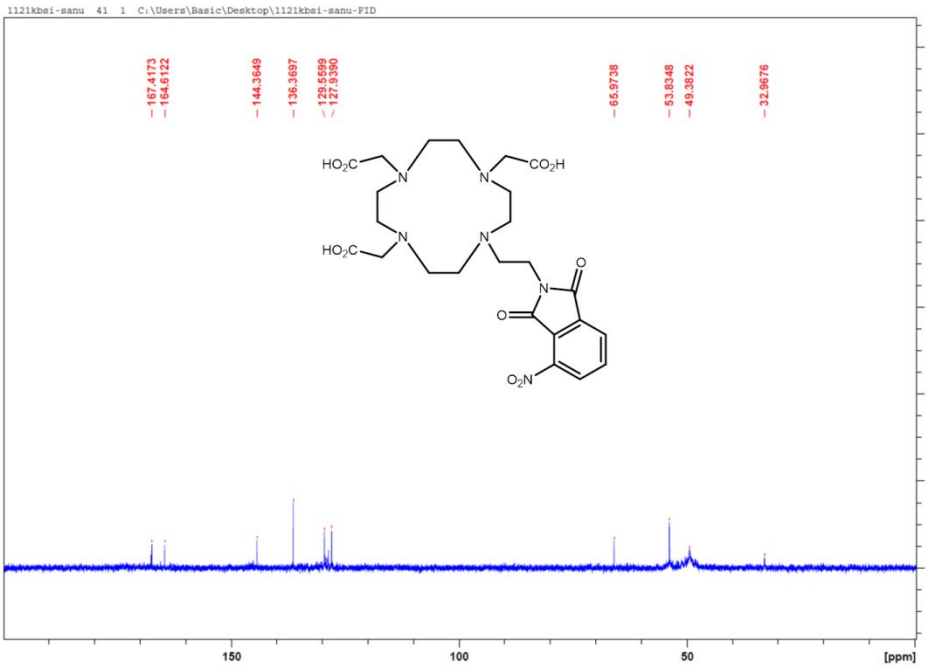

Figure S8. ^{13}C NMR spectrum of compound **4** in DMSO-d_6.

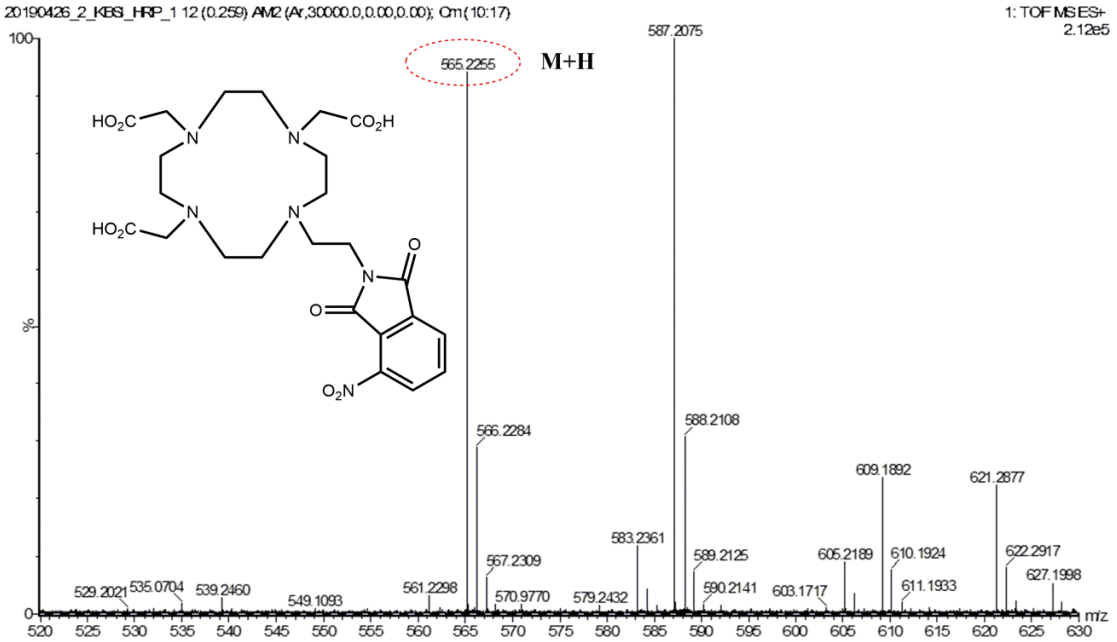

Figure S9. HRMS ESI spectrum of compound **4**.

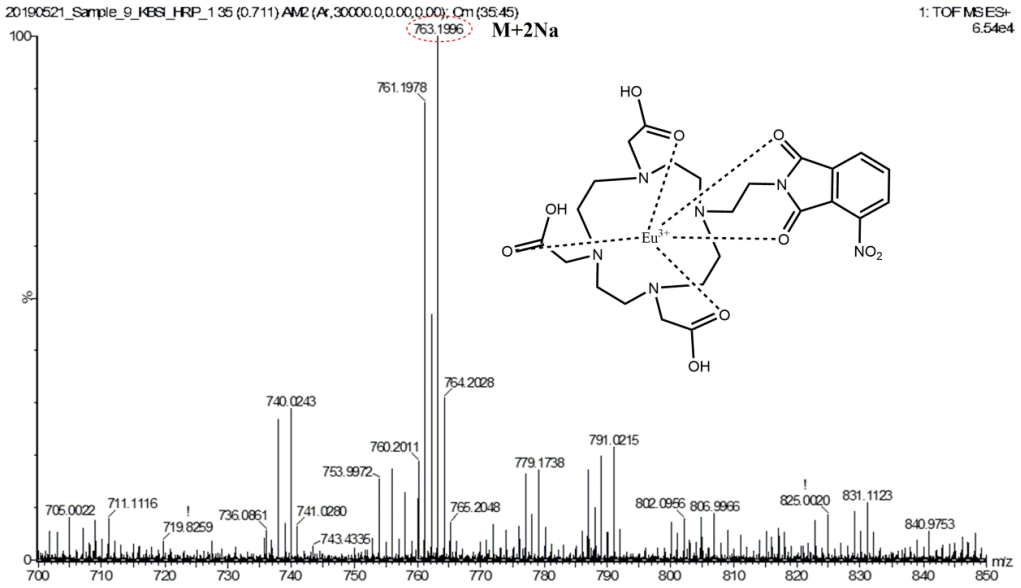

Figure S10. HRMS ESI spectrum of the **NO_2-Eu**.

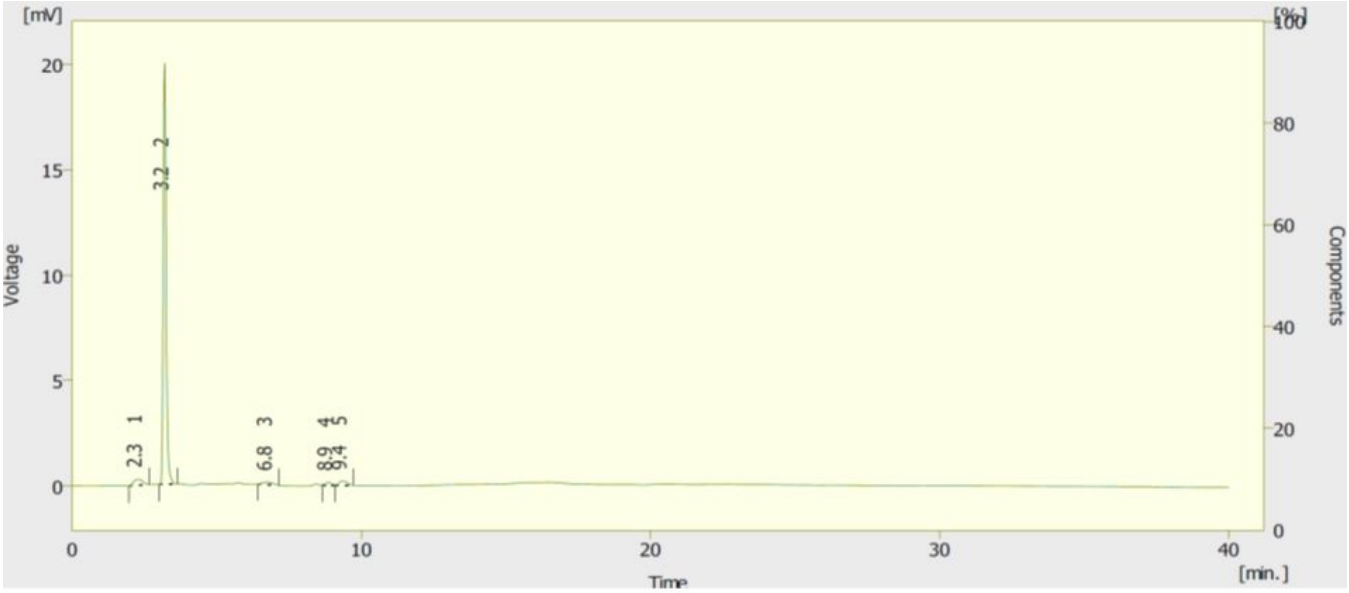

	Reten. Time [min]	Area [mV.s]	Height [mV]	Area [%]	Height [%]
1	2.277	3.271	0.286	2.3	1.4
2	3.200	135.890	19.960	95.2	96.3
3	6.770	1.658	0.127	1.1	0.6
4	8.860	0.536	0.146	0.4	0.7
5	9.360	1.437	0.206	1.0	1.0
	Total	142.792	20.725	100.0	100.0

Figure S11. HPLC spectrum of the **NO_2-Eu**. NO_2-Eu purity from this HPLC spectrum is 95.2%.

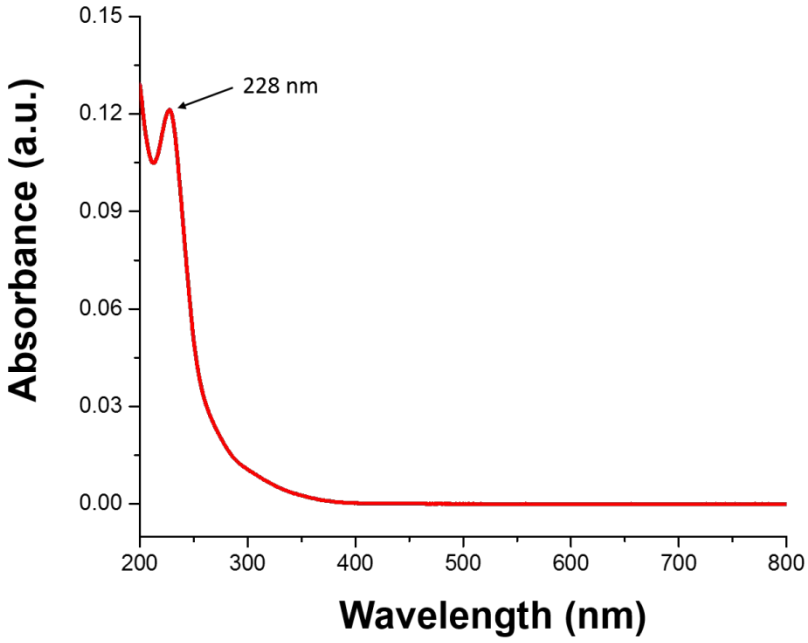

Figure S12. UV absorbance spectrum of **NO_2-Eu**.

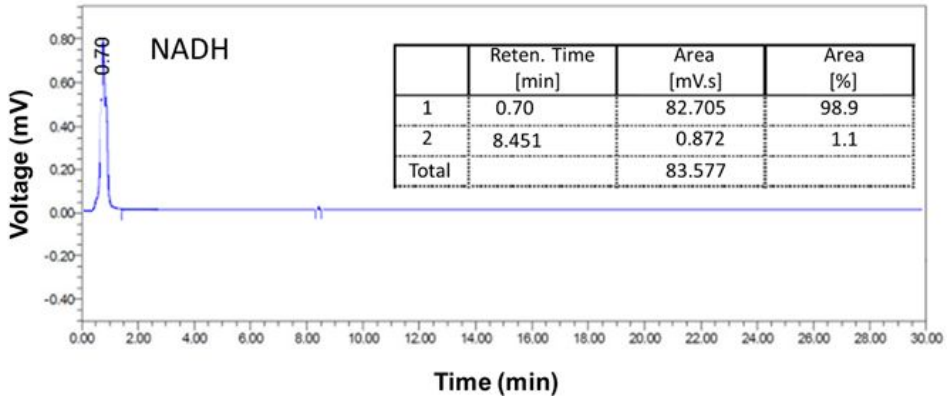

	Reten. Time [min]	Area [mV.s]	Area [%]
1	0.70	82.705	98.9
2	8.451	0.872	1.1
Total		83.577	

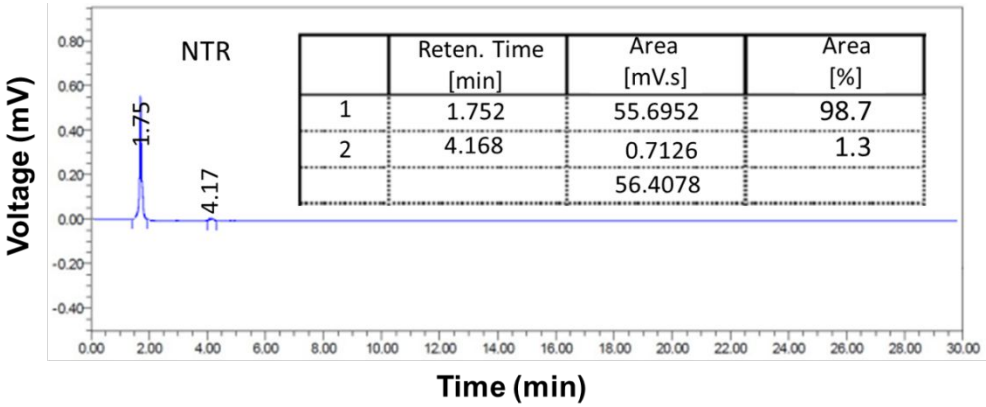

	Reten. Time [min]	Area [mV.s]	Area [%]
1	1.752	55.6952	98.7
2	4.168	0.7126	1.3
		56.4078	

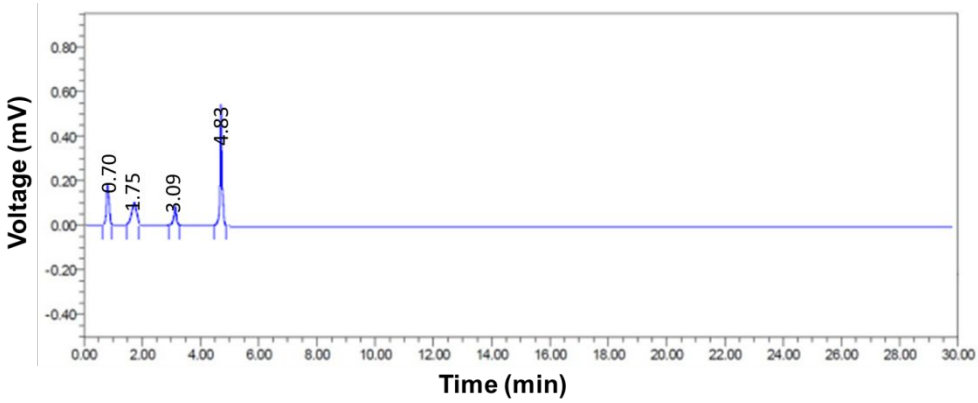

	Reten. Time [min]	Area [mV.s]	Area [%]
NADH	0.70	18.273	20.8
NTR	1.75	11.395	13.0
Eu-NO_2	3.09	5.614	6.4
Eu-NH_2	4.83	52.541	59.8
Total		87.823	

Figure S13. HPLC traces for lead compounds (**NO_2-Eu** treated with NTR and NADH).

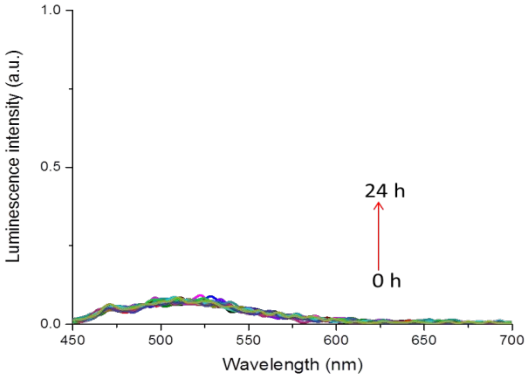

Figure S14. The stability of probe **NO_2-Eu** in media (DMEM + 10% FBS).

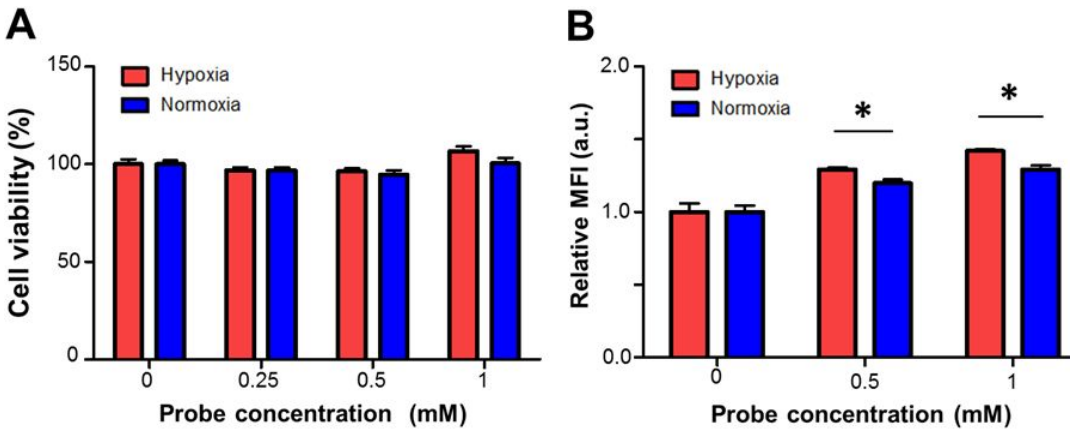

Figure S15. Cytotoxicity and luminescence profiles of probe NO_2-Eu at different concentrations under hypoxic and normoxic conditions. (A) Comparison of the cytotoxicity of probe **NO_2-Eu** in CT26 cancer cells under hypoxic (1% O_2) and normoxic (20% O_2) conditions for 3 h. (B) Mean luminescence intensity (MFI) values measured under the same conditions, as determined by flow cytometry. The data shown are averages of three independent experiments; error bars show the standard deviations. *$p < 0.05$.

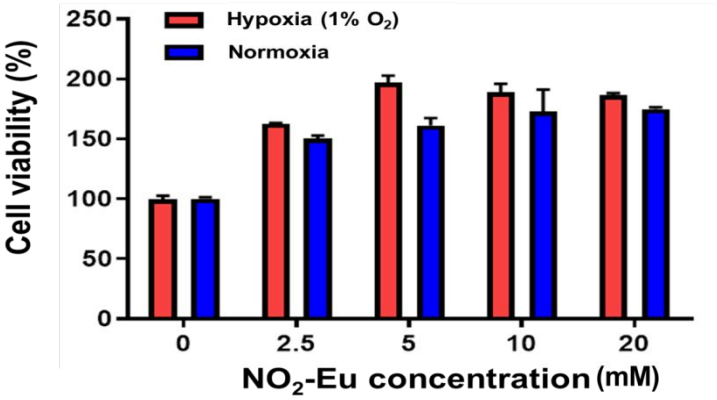

Figure S16. Cell viability of **NO_2-Eu** in CT26 cells under hypoxic (1% O_2) and normoxic (20% O_2) for 24 h. Note that the cell viability values higher than 100% are attributable to the relatively long 24 h incubation time.

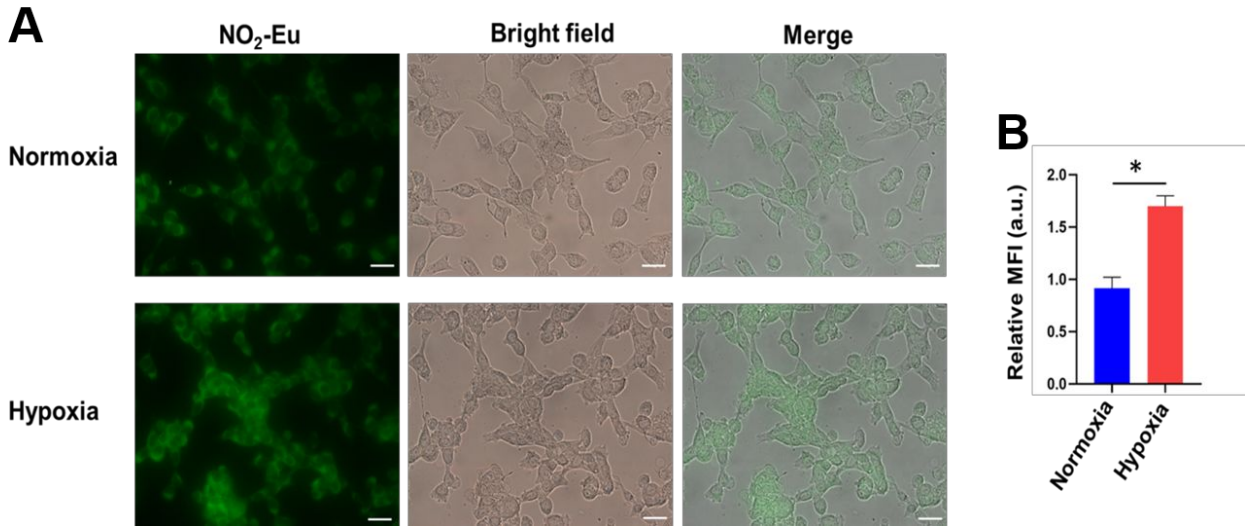

Figure S17. *In vitro* luminescence images (A) of CT26 cells incubated with **NO_2-Eu** (1 mM) for 30 min under normoxic (20% O_2) and hypoxic conditions (1% O_2), and a quantitative comparison (B).

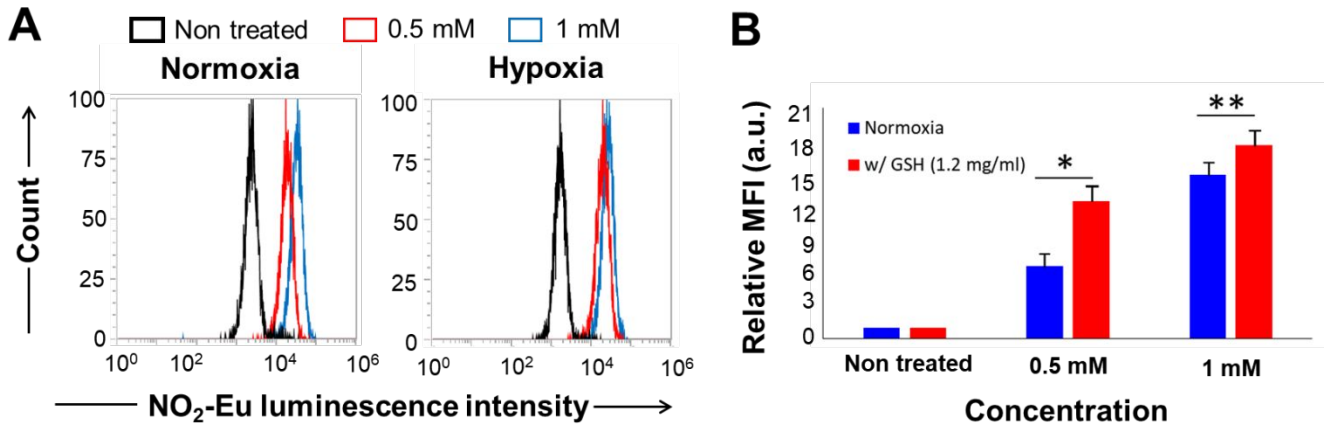

Figure S18. FACS analysis of CT26 cells incubated with different oxygen levels for 1.5 h only with **NO_2-Eu** (normoxia), antioxidant (1.2 mg/ml) and **NO_2-Eu** (hypoxia, 0.5 mM or 1 mM).

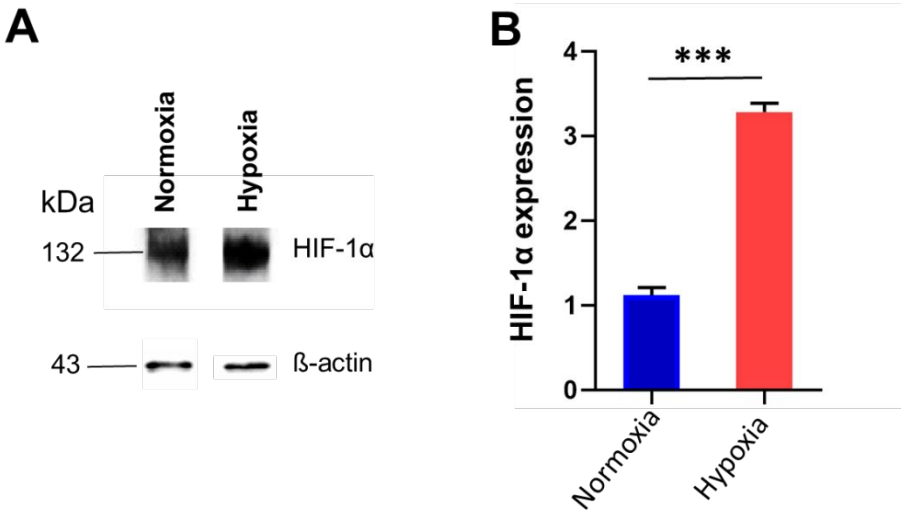

Figure S19. Western blot data analysis of hypoxia inducible factor-1α (HIF-1α) protein under normoxia (20% O_2) and hypoxia (1% O_2) condition in CT26 cells.

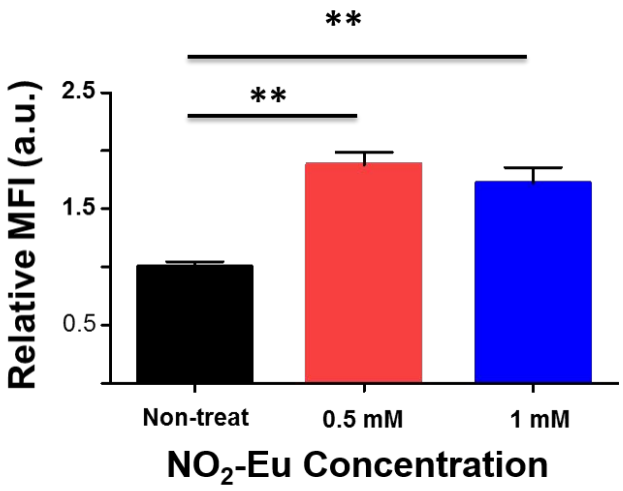

Figure S20. Luminescent intensity change of probe **NO_2-Eu** reacting with *Escherichia coli*, which was determined by FACS analysis.

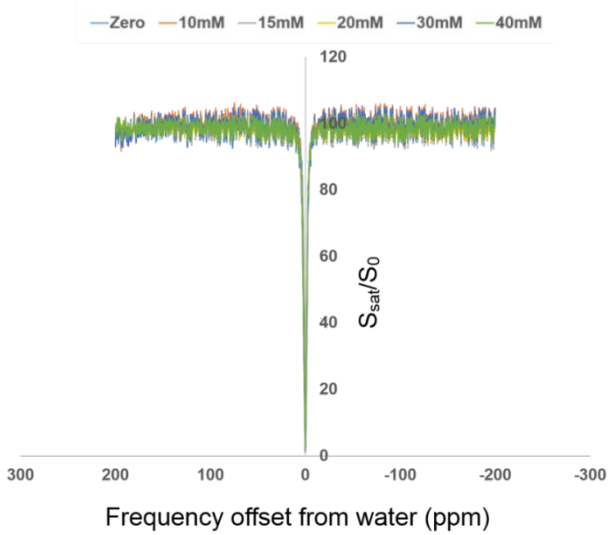

Figure S21. CEST MRI contrasts (z-spectra) recorded between +200 ppm and -200 ppm, depending on **NO_2-Eu** concentration (0, 10, 15, 20, 30, and 40 mM).

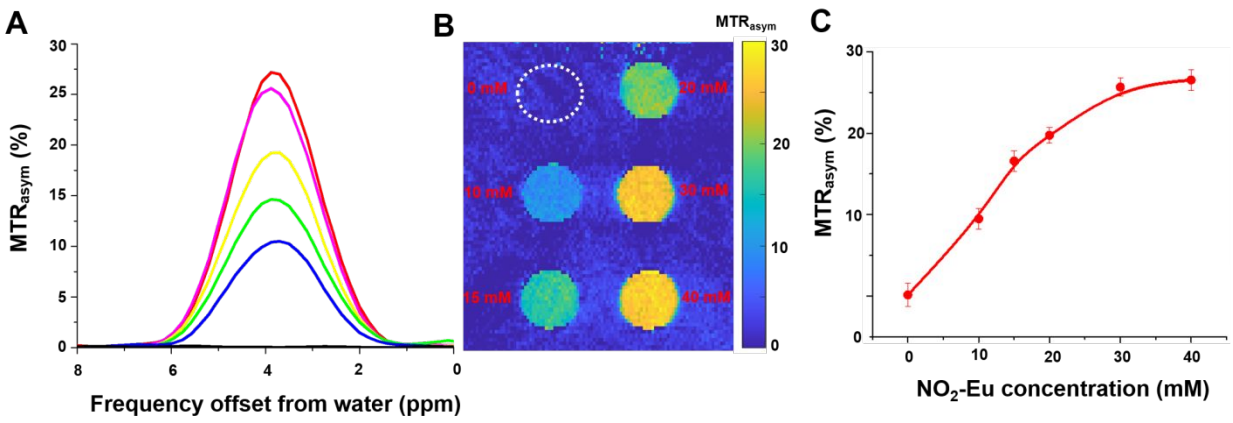

Figure S22. NO_2-Eu concentration dependence on the CEST effect. (A) MTR_{asym} (%) plot for various **NO_2-Eu** concentrations (from bottom to top; 0, 10, 15, 20, 30, and 40 mM) in PBS, following pre-incubation with 10 mM NTR for 60 min at 37°C and at pH 7.4. (B) A representative CEST color map at 4 ppm, and corresponding quantitative comparison (C) between the MTR_{asym} (%) value and the **NO_2-Eu** concentration. All experiments were carried out in the presence of NADH (200 μM).

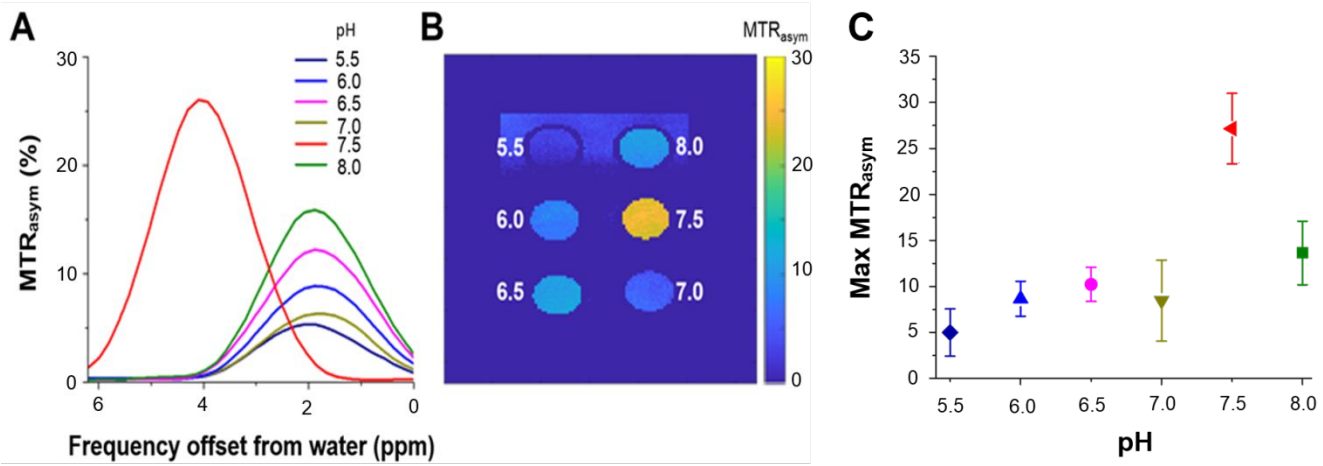

Figure S23. Effect of pH on the CEST contrast seen with the NO_2-Eu. (A) CEST spectra of probe **NO_2-Eu** (20 mM) containing 10 mM NTR recorded at different pH after equilibrating for 20 min in PBS. **(B)** CEST color map of solutions of probe **NO_2-Eu** at different pH. This CEST map reflects integration

over the 1.5–6.0 ppm frequency range. (C) Quantitative comparison of the maximum MTR_{asym} values measured from (A) as a function of pH.

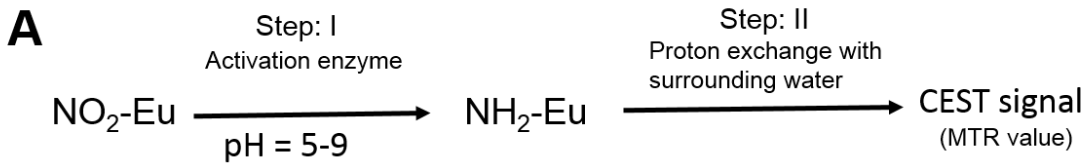

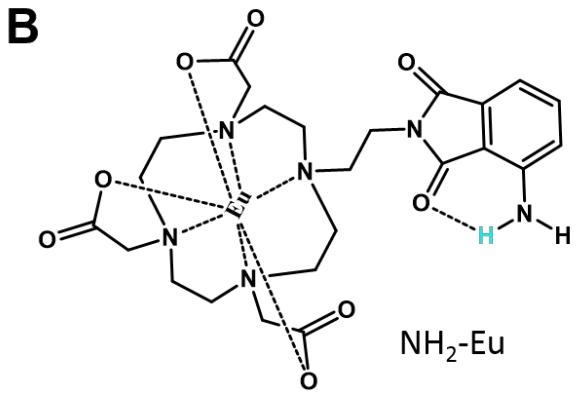

Scheme S2. (A) Two-step process of CEST enhancement. (B) Schematic view of the intramolecular hydrogen bonding expected to pertain at 7.4-7.5 pH in the activated agent (**NH_2-Eu**).

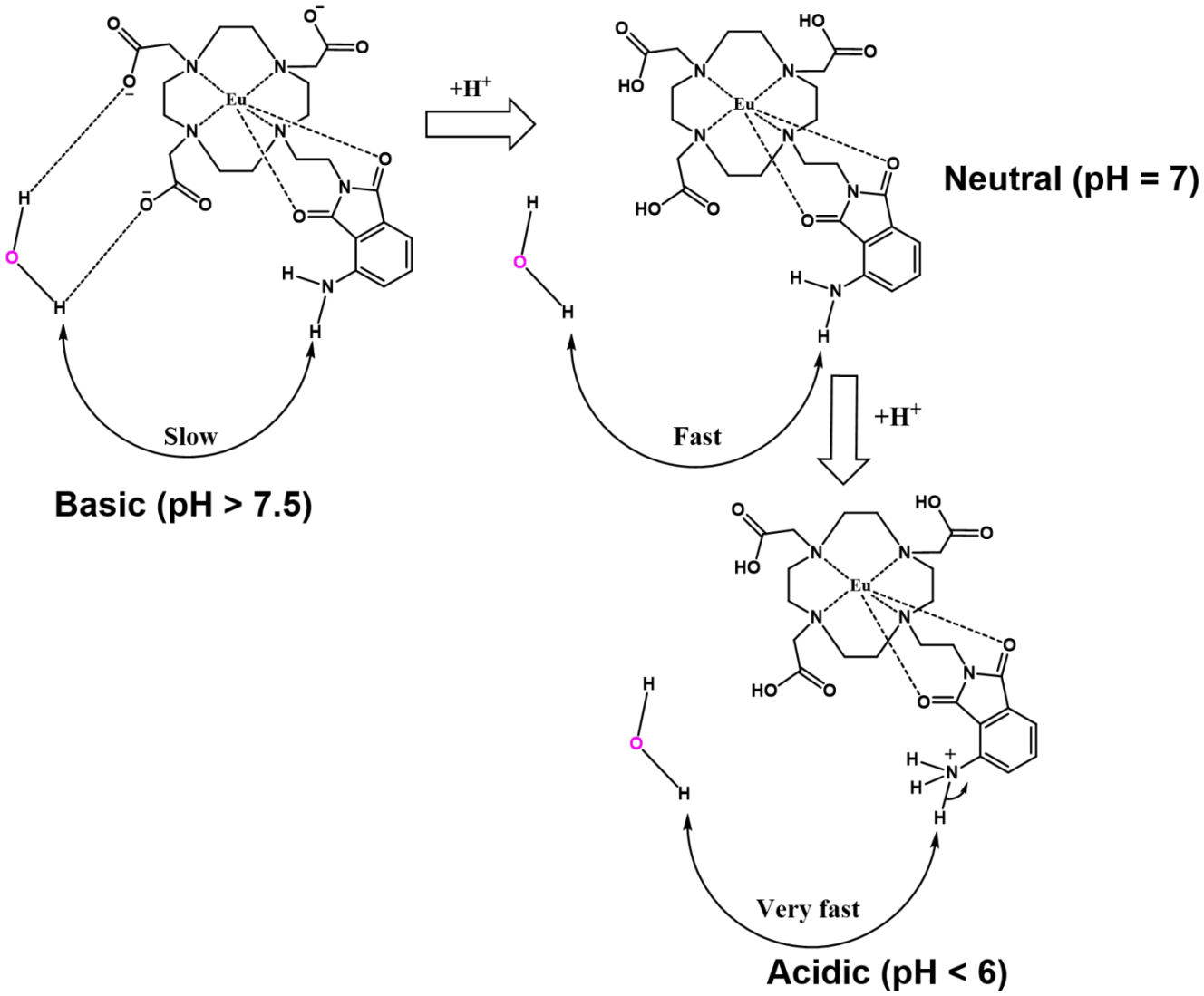

Scheme S3. Schematic of the prototropic effects on **NH_2-Eu** considered in this study. (Left) An ionized carboxyl group (CO_2^-) forms a strong hydrogen-bonding network with bulk water in basic medium (pH > 7.5) that slows prototropic exchange; therefore, a very strong CEST effect can be observed. (Right) Under neutral conditions where the carboxyl groups are protonated (e.g., pH ~7) a weaker hydrogen-bonding network is sustained, thereby allowing rapid proton exchange between bulk water protons and the protons on the $–NH_2$ molecules. As shown in the lower portion of the scheme, under acidic conditions, where the–

NH_2 groups are protonated (pH <6) fast proton exchange is expected, resulting in a very weak CEST effect.

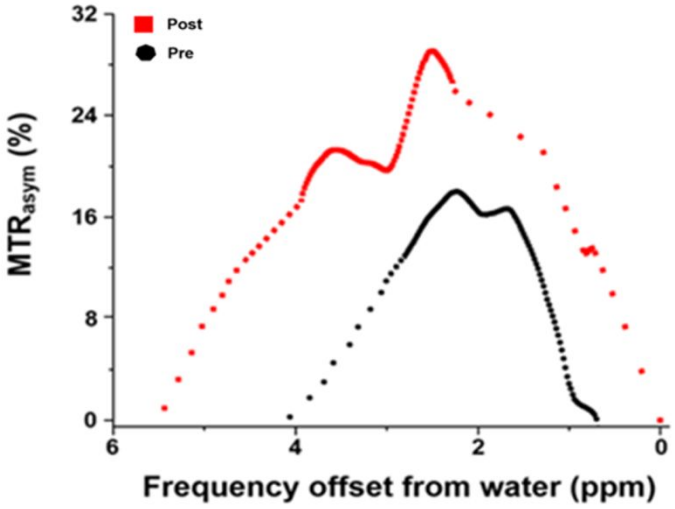

Figure S24. CEST MTR_{asym} spectra measured before and 1 h after the intra-tumoral injection of **NO_2-Eu** (50 mM).

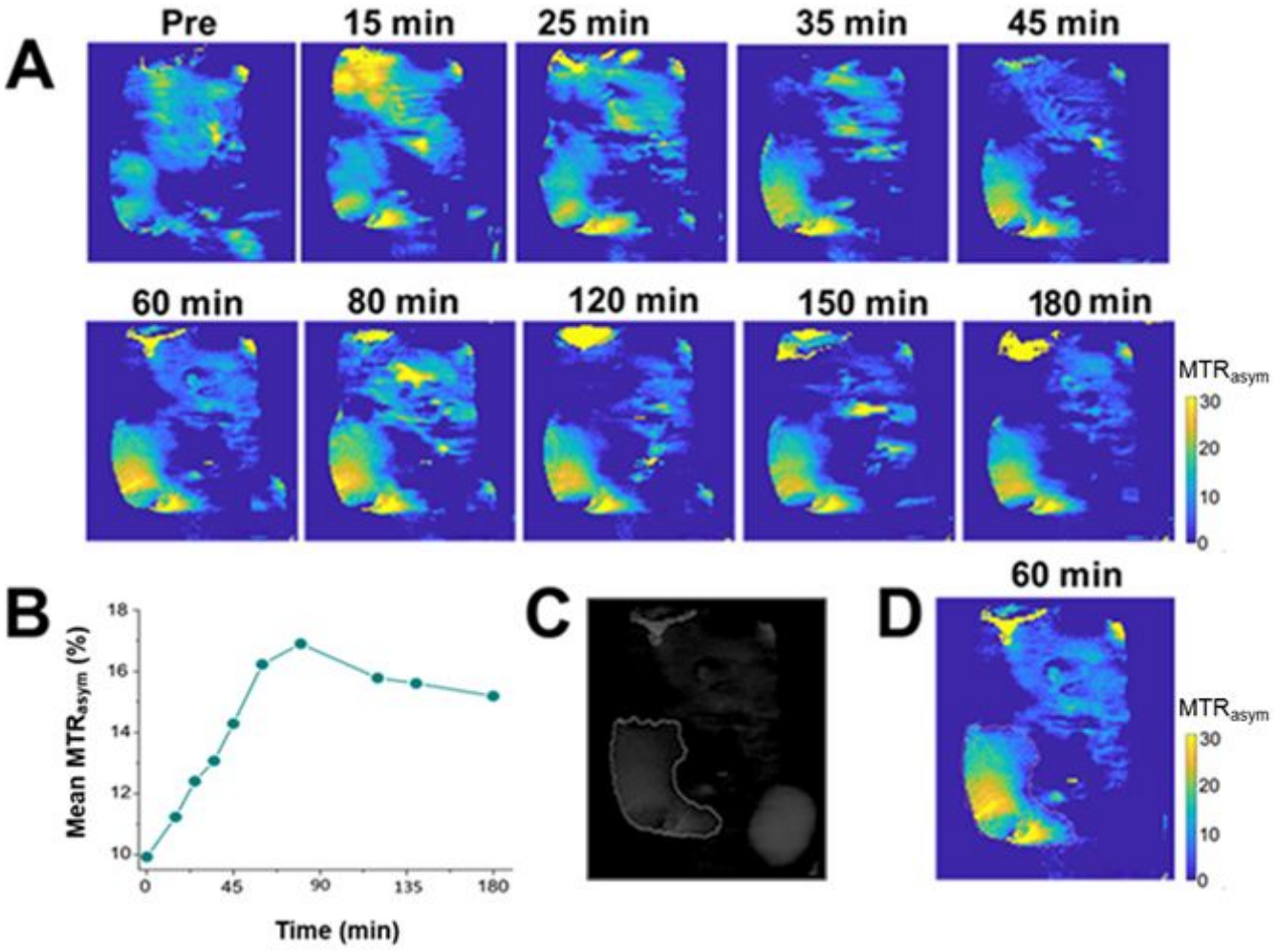

Figure S25. Time dependent *in vivo* CEST MR imaging at 2.5 ppm. (A) Time dependent *in vivo* CEST MR images of CT26 tumor bearing mouse were recorded before and after intratumoral injection (n = 3) of probe **NO_2-Eu** (50 mM, 100 μL) in PBS. The CEST MR images were calculated from the MTR_{asym} (%) values at 2.5 ppm. (B) Dynamic plot of the mean CEST intensity within entire tumor region (region-of-interests (ROIs) denoted in C and D) after injection of the **NO_2-Eu**. (C) T_2-weighted MR image indicating the tumor region (the white line defines the ROI), and (D) a corresponding CEST MR image.

Supplementary References

(1) Kim, M.; Gillen, J.; Landman, B. A.; Zhou, J.; van Zijl, P. C. Water saturation shift referencing (WASSR) for chemical exchange saturation transfer (CEST) experiments. *Magn. Reson. Med.* **2009**, *61*(6), 1441–1450.